

Thermal Buckling Analysis of Cross-Ply and Angle-Ply Laminated Composite Beam using Finite Element Method

Ms. Payal S. Shelke¹, Mr. Prabhuling Sarsambi², Dr. A.D.Desai³, Dr. S.D.Shinde⁴, Mr. M.D.Yelbhar⁵

¹ Student, Mechanical Engineering Department, SRES's Shree Ramchandra College of Engg., Maharashtra, India.

² Assistant Professor, Mechanical Engineering Department, SRES's Shree Ramchandra College of Engg., Maharashtra, India.

³ Principal, Mechanical Engineering Department, SRES's Shree Ramchandra College of Engg., Maharashtra, India.

⁴ Head of Department, Mechanical Engineering Department, SRES's Shree Ramchandra College of Engg., Maharashtra, India.

⁵ Assistant Professor, Civil Engineering Department, SRES's Shree Ramchandra College of Engg., Maharashtra, India.

ABSTRACT

Thermal buckling of thick, moderately thick and thin cross-ply and angle-ply laminated composite beams subjected to uniform temperature distribution are analyzed. The effects of length to thickness ratio and modulus ratio, various boundary conditions are used and numbers of layers on the critical buckling temperature are investigated. The finite element formulation is based on the first order shear deformation theory (FSDT). The finite element analysis has been carried out for a composite beam using an eight noded quadrilateral element. Numerical analysis has been carried out by developing APDL code in analysis software ANSYS and various results are obtained. The results are compared with those available in the literature. The present paper discusses the effect of number of layers, stacking sequence and boundary conditions on the buckling behavior of laminated composite beam with different ply orientations.

Keywords

Composite, cross-ply, angle-ply, thermal buckling, FSDT.

1. INTRODUCTION

Composite materials are engineered materials made from two or more constituent materials with significantly different physical or chemical properties which remain separate and distinct on a macroscopic level within the finished structure. They have varied applications including automobiles, army, aerospace, nuclear reactor vessels, turbines, buildings, smart highways as well as in sports equipment and medical prosthetics. Composites are being used increasingly for structural components of aircraft and space applications because of their superior specific strength and stiffness properties in comparison to conventional material. Buckling phenomenon is critically dangerous to structural components because the buckling of composite beam usually occurs at a lower applied stress and generates large deformation. The load at which buckling occurs depends on the stiffness of a component, not upon the strength of its materials. Buckling refers to the loss of stability of a component and is usually independent of material strength.

Marwah G. Kareem [1] analyzed the critical buckling temperature is dependent on the new displacement function field provided in the literature and uses third-order shear deformation theory. The value of the parameter "m," which determines the new displacement function, closed with the three-dimensional (3D) elasticity results. Thermal critical buckling is analyzed for thick and thin laminated plates by using the Navier solution for symmetric and anti-symmetric cross-ply simply supported boundary conditions. Several design parameters are considered such as extension thermal coefficient ratio (α_1/α_2), number of schemes, thickness ratio (a/h), aspect ratio (a/b), and modular ratio (E_1/E_2). Kapil Raje [2], investigated the use of finite element analysis to composite plate structures. The major purpose of this research is to use FEA techniques to evaluate the buckling behavior of composite plates. Fatima Zohra Kettaf et. Al [3], studied the mechanical and thermal buckling analysis of laminated composite plates is presented in this paper. Different theories of thick plates taking into account the parabolic distribution of transverse shear stresses and satisfying the condition of zero shear stresses on the top and bottom surfaces without using shear correction factor are presented. Akbas, Seref D. [4], investigated the thermal post-buckling analysis of a laminated composite beam subjected under uniform temperature rising with temperature dependent physical properties. The beam is pinned at both ends and immovable ends. Under temperature rising, thermal buckling and post-buckling phenomena occurs with immovable ends of the beam. Houdayfa Ounis et al [5] described the thermal buckling behavior of laminated composite plates: a finite element study. Rohit saha and Maiti. P. R [6] presented the buckling of simply supported FGM plates under uniaxial load. M. Kamruzzaman et al [7] studied the effect of composite type and its configuration on buckling strength of thin laminated composite plates. Erdogan Madenci and Ibrahim Guven [8] studied the finite element method and applications in engineering using ANSYS. A. Khdeir et al [9] studied the thermal buckling of cross-ply laminated composite beams.

Why composites are important:

Composite structures made of fibre reinforced composite are lighter than those made of conventional materials. In space vehicles, reduction in weight is linked to fuel savings. Spacecraft may have weight saving as much as forty percent if fibre reinforced composite structures are used. Coefficients of thermal expansion for many fibre reinforced composites are much lower than those of metals. As such composite structures exhibit a better dimensional stability over a wide range of temperature variation. However, differences in thermal expansion between metals and composite materials may create undue thermal stresses when they are used in conduction.

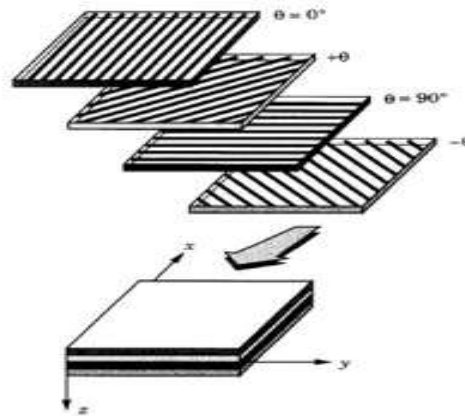


Figure 1: A laminate made up of laminae with different fibre orientations.

Composites can be very strength and stiffness, yet very light in weight, so ratios of strength-to-weight and stiffness-to-weight are several times greater than steel or aluminium. Fatigue properties are generally better than for common engineering metals. Toughness is often greater too. Composites can be designed that do not corrode like steel. Possible to achieve combinations of properties not attainable with metals, ceramics, or polymers alone. Corrosion resistance and durable. High specific strength and modulus, as well as high fatigue strength and fatigue damage tolerance.

2. FINITE ELEMENT METHOD AND FORMULATION

The first order shear deformation theory is considered in the finite element formulation. An eight noded isoparametric quadrilateral element is proposed for analysis of composite beam subjected to mechanical loading. The geometry and origin of the material coordinates are at the middle of the laminate as shown in Figure 2.

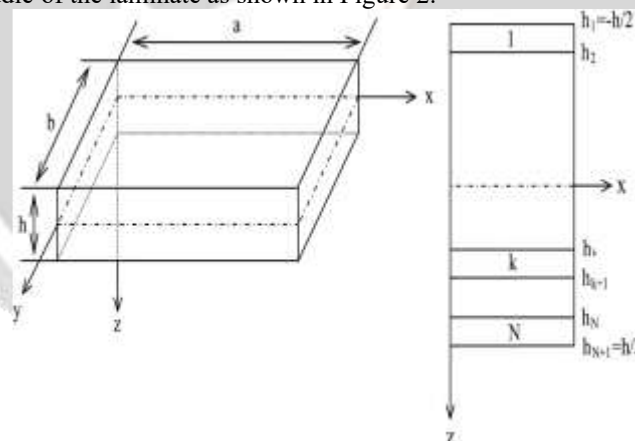


Figure 2: Geometry of the laminated composite beam.

2.1. Governing Equations

Consider a laminated beam of uniform thickness *t*, consisting of a number of thin laminae, each of which may be arbitrarily oriented at an angle *θ* with reference to the *x*-axis of the coordinate system (Figure. 1-2). The constitutive equations for the beam, when it is subjected to moisture and temperature, are given by

$$\{F\} = [D]\{\varepsilon\} - \{F^N\} \tag{1}$$

Where

$$\{F\} = \{N_x, N_y, N_{xy}, M_x, M_y, M_{xy}, Q_x, Q_y\}^T$$

$$\{F^N\} = \{N_x^N, N_y^N, N_{xy}^N, M_x^N, M_y^N, M_{xy}^N, 0, 0\}^T$$

$$\{\varepsilon\} = \{\bar{\varepsilon}_x, \bar{\varepsilon}_y, \bar{\gamma}_{xy}, k_x, k_y, k_{xy}, \phi_x, \phi_y\}^T$$

$$[D] = \begin{bmatrix} A_{11} & A_{12} & A_{16} & B_{11} & B_{12} & B_{16} & 0 & 0 \\ A_{12} & A_{22} & A_{26} & B_{12} & B_{22} & B_{26} & 0 & 0 \\ A_{16} & A_{26} & A_{66} & B_{16} & B_{26} & B_{66} & 0 & 0 \\ B_{11} & B_{12} & B_{16} & D_{11} & D_{12} & D_{16} & 0 & 0 \\ B_{12} & B_{22} & B_{26} & D_{12} & D_{22} & D_{26} & 0 & 0 \\ B_{16} & B_{26} & B_{66} & D_{16} & D_{26} & D_{66} & 0 & 0 \\ 0 & 0 & 0 & 0 & 0 & 0 & A_{44} & A_{45} \\ 0 & 0 & 0 & 0 & 0 & 0 & A_{45} & A_{55} \end{bmatrix}$$

The non-mechanical force and moment resultants are given by

$$\{N_x^N, N_y^N, N_{xy}^N\}^T = \sum_{k=1}^n \int_{z_{k-1}}^{z_k} [\bar{Q}_{ij}]_k \{e\}_k dz \quad (i, j = 1, 2, 6) \tag{2}$$

$$\{M_x^N, M_y^N, M_{xy}^N\}^T = \sum_{k=1}^n \int_{z_{k-1}}^{z_k} [\bar{Q}_{ij}]_k \{e\}_k z dz$$

Where $\{e\}_k = \{e_x, e_y, e_{xy}\}^T = [T] \{\beta_1, \beta_2\}_k^T (C - C_0) + [T] \{\alpha_1, \alpha_2\}_k^T (T - T_0)$ in which

$$[T] = \begin{bmatrix} \cos^2 \theta & \sin^2 \theta \\ \sin^2 \theta & \cos^2 \theta \\ \sin 2\theta & -\sin 2\theta \end{bmatrix}$$

The stiffness coefficients are defined as

$$(A_{ij}, B_{ij}, D_{ij}) = \sum_{k=1}^n \int_{z_{k-1}}^{z_k} [\bar{Q}_{ij}]_k (1, z, z^2) dz \quad (i, j = 1, 2, 6) \tag{3}$$

$$(A_{ij}) = \alpha \sum_{k=1}^n \int_{z_{k-1}}^{z_k} [\bar{Q}_{ij}]_k dz \quad (i, j = 4, 5)$$

$[\bar{Q}_{ij}]_k$ in eqns (2) and (3) is defined as $[\bar{Q}_{ij}]_k = [T_1]^{-1} [Q_{ij}]_k [T_1]^{-T} \quad (i, j = 1, 2, 6)$

$$[\bar{Q}_{ij}]_k = [T_2]^{-1} [Q_{ij}]_k [T_2] \quad (i, j = 4, 5) \tag{4}$$

Where $[T_1] = \begin{bmatrix} \cos^2 \theta & \sin^2 \theta & 2 \sin \theta \cos \theta \\ \sin^2 \theta & \cos^2 \theta & -2 \sin \theta \cos \theta \\ -\sin \theta \cos \theta & \sin \theta \cos \theta & \cos^2 \theta - \sin^2 \theta \end{bmatrix} \quad [T_2] = \begin{bmatrix} \cos \theta & -\sin \theta \\ \sin \theta & \cos \theta \end{bmatrix}$

$$[Q_{ij}]_k = \begin{bmatrix} Q_{11} & Q_{12} & 0 \\ Q_{12} & Q_{22} & 0 \\ 0 & 0 & Q_{66} \end{bmatrix} \quad (i, j = 1, 2, 6)$$

$$[Q_{ij}]_k = \begin{bmatrix} Q_{44} & 0 \\ 0 & Q_{55} \end{bmatrix} \quad (i, j = 4, 5)$$

In which

$$Q_{11} = E_1 / (1 - \nu_{12} \nu_{21})$$

$$Q_{12} = \nu_{12} E_2 / (1 - \nu_{12} \nu_{21}) \quad Q_{55} = G_{23}$$

$$Q_{22} = E_2 / (1 - \nu_{12} \nu_{21})$$

$$Q_{44} = G_{13}$$

And $Q_{66} = G_{12}$

The linear strains are defined as

$$\bar{\epsilon}_x = \bar{u}_{,x}, \bar{\epsilon}_y = \bar{v}_{,y}, \bar{\gamma}_{xy} = \bar{u}_{,y} + \bar{v}_{,x}, K_x = \theta_{y,x}, K_y = -\theta_{x,y}$$

$$K_{xy} = \theta_{y,y} - \theta_{x,x}, \phi_x = \theta_y + w_x \text{ and } \phi_y = -\theta_x - w_y \tag{5}$$

Assuming that w does not vary with z , the non-linear strains of the beam can be expressed as

$$\begin{aligned}
 \epsilon_{xnl} &= (\mathbf{u}_x^2 + \mathbf{v}_x^2 + \mathbf{w}_x^2) / 2 \\
 \epsilon_{ynl} &= (\mathbf{u}_y^2 + \mathbf{v}_y^2 + \mathbf{w}_y^2) / 2 \\
 \gamma_{xynl} &= (\mathbf{u}_x \mathbf{u}_y + \mathbf{v}_x \mathbf{v}_y + \mathbf{w}_x \mathbf{w}_y) \\
 \gamma_{xznl} &= (\mathbf{u}_x \mathbf{u}_z + \mathbf{v}_x \mathbf{v}_z) \\
 \gamma_{yznl} &= (\mathbf{u}_y \mathbf{u}_z + \mathbf{v}_y \mathbf{v}_z)
 \end{aligned} \tag{6}$$

Since $\mathbf{u} = \bar{\mathbf{u}} + z\boldsymbol{\theta}_y$ and $\mathbf{v} = \bar{\mathbf{v}} - z\boldsymbol{\theta}_x$, eqns (6) may be written as

$$\epsilon_{xnl} = \left[\begin{array}{c} \bar{\mathbf{u}}_x^2 + \bar{\mathbf{v}}_x^2 + \mathbf{w}_x^2 + 2z(\bar{\mathbf{u}}_x \boldsymbol{\theta}_{y,x} - \bar{\mathbf{v}}_x \boldsymbol{\theta}_{x,x}) \\ + z^2 (\boldsymbol{\theta}_{y,x}^2 + \boldsymbol{\theta}_{x,x}^2) \end{array} \right] / 2$$

$$\begin{aligned}
 \epsilon_{ynl} &= \left[\begin{array}{c} \bar{\mathbf{u}}_y^2 + \bar{\mathbf{v}}_y^2 + \mathbf{w}_y^2 + 2z(\bar{\mathbf{u}}_y \boldsymbol{\theta}_{y,y} - \bar{\mathbf{v}}_y \boldsymbol{\theta}_{x,y}) \\ + z^2 (\boldsymbol{\theta}_{x,y}^2 + \boldsymbol{\theta}_{y,y}^2) \end{array} \right] / 2 \\
 \gamma_{xynl} &= \left[\begin{array}{c} \bar{\mathbf{u}}_x \bar{\mathbf{u}}_y + \bar{\mathbf{v}}_x \bar{\mathbf{v}}_y + \mathbf{w}_x \mathbf{w}_y + z(\bar{\mathbf{u}}_y \boldsymbol{\theta}_{y,x} - \bar{\mathbf{u}}_x \boldsymbol{\theta}_{y,y}) \\ -z(\bar{\mathbf{v}}_y \boldsymbol{\theta}_{x,x} + \bar{\mathbf{v}}_x \boldsymbol{\theta}_{x,y}) + z^2 (\boldsymbol{\theta}_{y,x} \boldsymbol{\theta}_{y,y} + \boldsymbol{\theta}_{x,x} \boldsymbol{\theta}_{x,y}) \end{array} \right] \\
 \gamma_{xznl} &= \left[\bar{\mathbf{u}}_x \boldsymbol{\theta}_y - \bar{\mathbf{v}}_x \boldsymbol{\theta}_x + z(\boldsymbol{\theta}_y \boldsymbol{\theta}_{y,x} + \boldsymbol{\theta}_x \boldsymbol{\theta}_{x,x}) \right] \\
 \gamma_{yznl} &= \left[\bar{\mathbf{u}}_y \boldsymbol{\theta}_y - \bar{\mathbf{v}}_y \boldsymbol{\theta}_x + z(\boldsymbol{\theta}_y \boldsymbol{\theta}_{y,y} + \boldsymbol{\theta}_x \boldsymbol{\theta}_{x,y}) \right]
 \end{aligned} \tag{7}$$

2.2. Isoparametric Element

In the present analysis eight-noded quadrilateral isoparametric element with five degrees of freedom \mathbf{u} , \mathbf{v} , \mathbf{w} , $\boldsymbol{\theta}_x$, and $\boldsymbol{\theta}_y$ is used and as shown in Figure 3. The beam is discretized into finite element, the shape functions of the element are given by

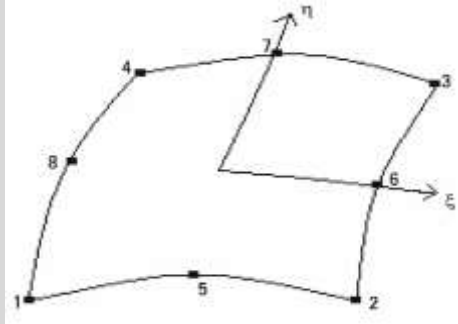


Figure 3: Doubly curved eight noded isoparametric elements.

$$\begin{aligned}
 N_1 &= \frac{1}{4}(1-\xi)(1-\eta)(-\xi-\eta-1) \\
 N_2 &= \frac{1}{4}(1+\xi)(1-\eta)(\xi-\eta-1) \\
 N_3 &= \frac{1}{4}(1+\xi)(1+\eta)(\xi+\eta-1) \\
 N_4 &= \frac{1}{4}(1-\xi)(1+\eta)(-\xi+\eta-1) \\
 N_5 &= \frac{1}{2}(1-\xi^2)(1-\eta) \\
 N_6 &= \frac{1}{2}(1+\xi^2)(1-\eta^2) \\
 N_7 &= \frac{1}{2}(1-\xi^2)(1+\eta) \\
 N_8 &= \frac{1}{2}(1-\xi)(1+\eta^2)
 \end{aligned}$$

The local coordinates of the elements are ξ and η for the isoparametric quadrilateral elements are represented by the interpolation functions.

$$\bar{u} = \sum_{i=1}^8 N_i \bar{u}_i, \quad \bar{v} = \sum_{i=1}^8 N_i \bar{v}_i, \quad w = \sum_{i=1}^8 N_i w_i, \quad (8) \quad \theta_x = \sum_{i=1}^8 N_i \theta_{xi},$$

$$\theta_y = \sum_{i=1}^8 N_i \theta_{yi},$$

2.3. Stiffness Matrix

The linear strain matrix (ϵ) for an element is obtained by substituting eqns (8) into (5). It is expressed as

$$(\epsilon) = [B] \{ \delta_e \} \quad (9)$$

Where $\{ \delta_e \} = \{ \bar{u}_1, \bar{v}_1, w_1, \theta_{x1}, \theta_{y1}, \dots, \bar{u}_8, \bar{v}_8, w_8, \theta_{x8}, \theta_{y8} \}^T$

$$[B] = \sum_{i=1}^8 \begin{bmatrix} N_{i,x} & 0 & 0 & 0 & 0 \\ 0 & N_{i,y} & 0 & 0 & 0 \\ N_{i,y} & N_{i,x} & 0 & 0 & 0 \\ 0 & 0 & 0 & 0 & N_{i,x} \\ 0 & 0 & 0 & -N_{i,y} & 0 \\ 0 & 0 & 0 & -N_{i,x} & N_{i,y} \\ 0 & 0 & N_{i,x} & 0 & N_i \\ 0 & 0 & N_{i,y} & -N_i & 0 \end{bmatrix}$$

The element stiffness matrix is given by $[K_e] = \iint [B]^T [D][B] dx dy$ (10)

2.4. Geometric stiffness matrix $[K_{Ge}^\alpha]$

The first three non-linear strains in eqns (7) are represented in a matrix form

$$\{ \epsilon_{xnl}, \epsilon_{ynl}, \gamma_{xy nl} \}^T = [U] \{ f \} / 2 \quad (11)$$

Where $\{ f \} = \{ \bar{u}_x, \bar{u}_y, \bar{v}_x, \bar{v}_y, w_x, w_y, \theta_{xx}, \theta_{xy}, \theta_{yx}, \theta_{yy} \}^T$ (12)

And $[U]$ is obvious from the expressions for $\epsilon_{xnl}, \epsilon_{ynl}, \gamma_{xy nl}$ and eqn (11) Using eqn (8) is put into eqn (12), and $\{ f \}$ is expressed as

$$\{ f \} = [H] \{ \delta_e \} \quad (13)$$

Where

$$[H] = \sum_{i=1}^8 \begin{bmatrix} N_{i,x} & 0 & 0 & 0 & 0 \\ N_{i,y} & 0 & 0 & 0 & 0 \\ 0 & N_{i,x} & 0 & 0 & 0 \\ 0 & N_{i,y} & 0 & 0 & 0 \\ 0 & 0 & N_{i,x} & 0 & 0 \\ 0 & 0 & N_{i,y} & 0 & 0 \\ 0 & 0 & 0 & N_{i,x} & 0 \\ 0 & 0 & 0 & N_{i,y} & 0 \\ 0 & 0 & 0 & 0 & N_{i,x} \\ 0 & 0 & 0 & 0 & N_{i,y} \end{bmatrix}$$

The geometric stiffness matrix due to applied in-plane loads is given by: $[K_{Ge}^\alpha] = \iint [H]^T [P][H] dx dy$ (14)

Where

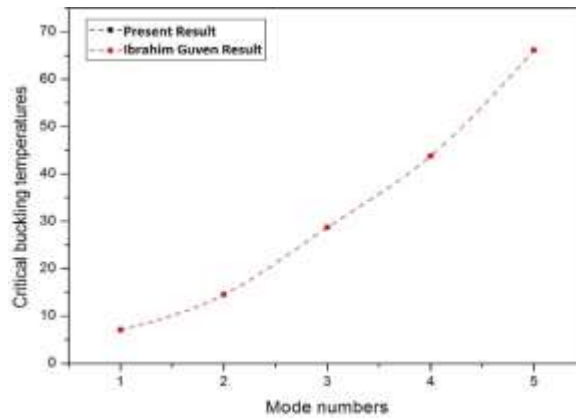


Figure 4: Comparison of the present result Ibrahim Guven result for clamped beam.

Table 1: Material properties (graphite-epoxy) of non-dimensional thermal buckling of beams.

Engineering constants	Orthotropic material properties
E_1	358GPa
$E_2 = E_3$	17.9GPa
$G_{12} = G_{13}$	0.6GPa
G_{23}	0.5GPa
ν_{12}	0.25
$\nu_{23} = \nu_{13}$	0.0125
α_1	3e-6
α_2	9e-6
h	1

Table 2: Non-dimensional first critical buckling temperature, $\bar{T}_{cr} = T_{cr} \alpha_1 (L/h)^2$ of clamped-clamped anti-symmetric cross-ply (0/90) beams, for different length to thickness ratios.

L/h	Number of Layers (n)		
	n=2	n=4	n=10
5	0.518813	0.700013	0.72759
10	0.87555	1.51935	1.6542
20	1.062552	2.15016	2.427
30	1.106865	2.329641	2.656989
40	1.123344	2.3999808	2.748144
50	1.13115	2.433825	2.79245

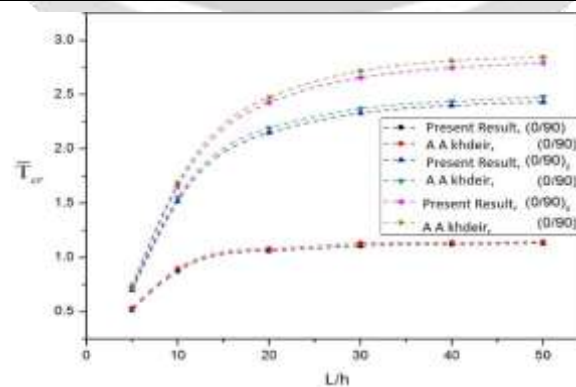


Figure 5: Effect of length to thickness ratio (L/h) on the non-dimensional first critical buckling temperature anti-symmetric cross-ply (0/90) clamped-clamped beams having different number of layers.

Represents the figure 5, thermal buckling analysis of laminated composite beam subjected to uniform temperature distribution, the effect of coupling is to increase the non-dimensional critical buckling temperature with the increase in the length to thickness

ratio (L/h) and. The first buckling mode is the one requiring the smallest non-dimensional critical buckling temperature. As goes on increasing the length to thickness ratio and increasing the non-dimensional critical buckling load and the number of layers increases the non-dimensional critical buckling temperatures also increase.

3.2. Numerical Examples

In the present analysis study the effect of number of layers on stacking sequence of laminated composite beams and clamped boundary conditions is examined for anti-symmetric and symmetric cross-ply and angle ply laminates. Numerical problems are carried out for different length to thickness ratio and modulus ratio with clamped boundary conditions. Now considering the thermal buckling analysis is carried out for orthotropic material (graphite-epoxy) are analyzed in which clamped boundary conditions on both edges under uniform temperature distribution (26⁰ Kelvin) and material properties are given in above Table 1.

Table 3: Non-dimensional first critical buckling temperature, $\bar{T}_{cr} = T_{cr} \alpha_1 (L/h)^2$ of clamped-clamped anti-symmetric angle-ply (15/-15)_n beams, for different length to length to thickness ratios.

L/h	Number of Layers (n)				
	(15/-15)	(15/-15) ₂	(15/-15) ₃	(15/-15) ₄	(15/-15) ₅
5	0.673358	0.68649	0.68175	0.67986	0.678953
10	1.54374	1.73928	1.75341	1.75725	1.75887
20	2.3238	2.79828	2.85492	2.87304	2.8812
30	2.58468	3.159	3.23136	3.25512	3.26565
40	2.69943	3.31114	3.389424	3.415008	3.426528
50	2.75295	3.3855	3.4671	3.493875	3.505875

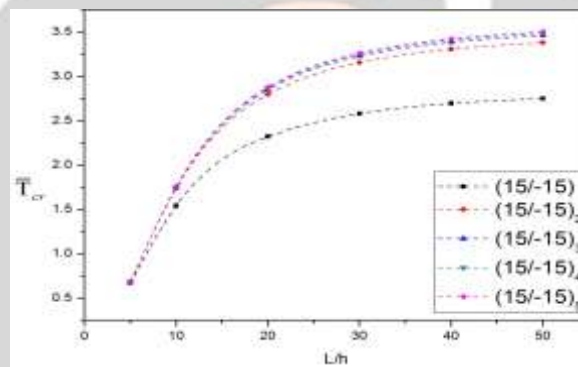


Figure 6: Effect of length to thickness ratio (L/h) on the non-dimensional first critical buckling temperature anti-symmetric angle-ply (15/-15)_n clamped-clamped beams having different number of layers.

Table 4: Non-dimensional first critical buckling temperature, $\bar{T}_{cr} = T_{cr} \alpha_1 (L/h)^2$ of clamped-clamped anti-symmetric angle-ply (30/-30)_n beams, for different length to length to thickness ratios.

L/h	Number of Layers (n)				
	(30/-30)	(30/-30) ₂	(30/-30) ₃	(30/-30) ₄	(30/-30) ₅
5	1.252275	1.44375	1.45065	1.4514	1.4514
10	2.25639	2.9163	2.98068	3.0009	3.0009
20	2.8332	3.81108	3.91608	3.94956	3.94956
30	2.98404	4.03974	4.15476	4.19148	4.20795
40	3.048048	4.13088	4.249344	4.287264	4.304256
50	3.074175	4.170675	4.2902	4.329375	4.346625

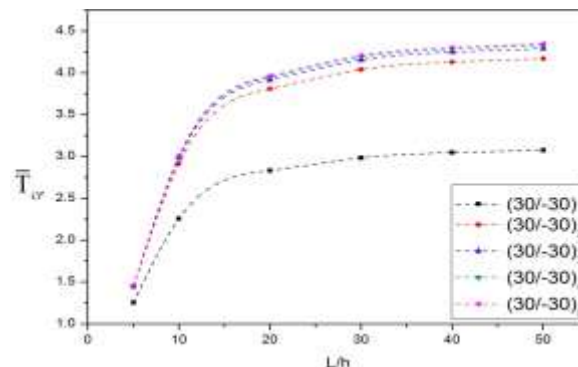


Figure 7: Effect of length to thickness ratio (L/h) on the non-dimensional first critical buckling temperature anti-symmetric angle-ply (30/-30)_n clamped-clamped beams having different number of layers.

Table 5: Non-dimensional first critical buckling temperature, $\bar{T}_{cr} = T_{cr} \alpha_1 (L/h)^2$ of clamped-clamped anti-symmetric angle-ply (45/-45)_n beams, for different length to length to thickness ratios.

L/h	Number of Layers (n)				
	(45/-45) ₁	(45/-45) ₂	(45/-45) ₃	(45/-45) ₄	(45/-45) ₅
5	1.40835	1.69305	1.720425	1.72905	1.732875
10	2.00181	2.45583	2.50086	2.51511	2.52147
20	2.23704	2.74632	2.79696	2.81292	2.82012
30	2.288844	2.80692	2.85849	2.87469	2.88198
40	2.309904	2.829504	2.87928	2.89488	2.90184
50	2.31795	2.838	2.88735	2.90295	2.909925

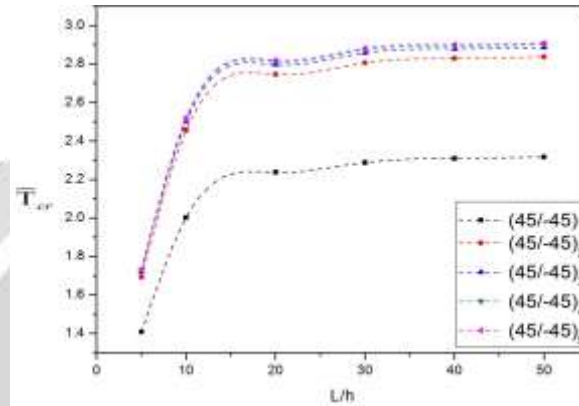


Figure 8: Effect of length to thickness ratio (L/h) on the non-dimensional first critical buckling temperature anti-symmetric angle-ply (45/-45)_n clamped-clamped beams having different number of layers.

Table 6: Non-dimensional first critical buckling temperature, $\bar{T}_{cr} = T_{cr} \alpha_1 (L/h)^2$ of clamped-clamped anti-symmetric angle-ply (60/-60)_n beams, for different length to length to thickness ratios.

L/h	Number of Layers (n)				
	(60/-60) ₁	(60/-60) ₂	(60/-60) ₃	(60/-60) ₄	(60/-60) ₅
5	1.053825	1.116525	1.12245	1.124325	1.12515
10	1.33782	1.41831	1.42584	1.42824	1.42929
20	1.4346	1.51824	1.52592	1.52832	1.5294
30	1.454544	1.53819	1.545858	1.548261	1.549341
40	1.462128	1.545312	1.552656	1.554912	1.555872
50	1.465425	1.54845	1.555575	1.557825	1.5588

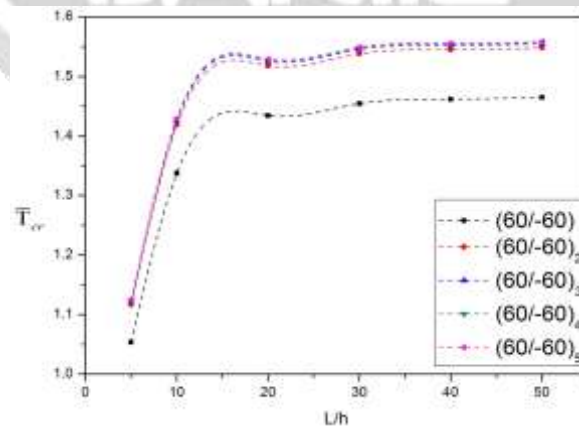


Figure 9: Effect of length to thickness ratio (L/h) on the non-dimensional first critical buckling temperature anti-symmetric angle-ply (60/-60)_n clamped-clamped beams having different number of layers.

Table 7: Non-dimensional first critical buckling temperature, $\bar{T}_{cr} = T_{cr} \alpha_1 (L/h)^2$ of clamped-clamped anti-symmetric angle-ply (75/-75)_n beams, for different length to length to thickness ratios.

L/h	Number of Layers (n)				
	(75/-75)	(75/-75) ₂	(75/-75) ₃	(75/-75) ₄	(75/-75) ₅
5	0.873825	0.88005	0.880725	0.880875	0.88095
10	1.07391	1.08285	1.08381	1.08411	1.08426
20	1.139688	1.149672	1.150788	1.151148	1.151304
30	1.153035	1.163268	1.164429	1.164807	1.164969
40	1.157952	1.168368	1.16952	1.169904	1.170096
50	1.160175	1.1706	1.1718	1.172175	1.172325

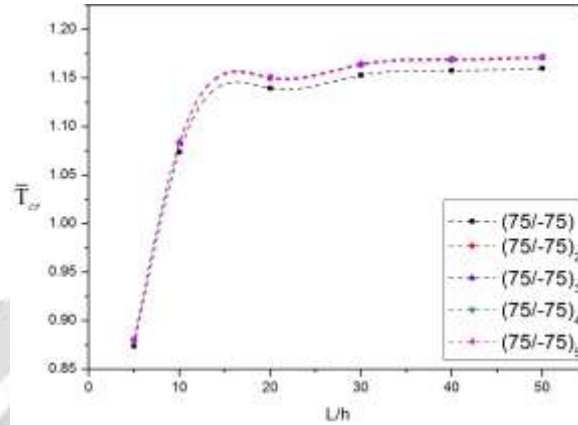


Figure 10: Effect of length to thickness ratio (L/h) on the non-dimensional first critical buckling temperature anti-symmetric angle-ply (75/-75)_n clamped-clamped beams having different number of layers.

Table 8: Non-dimensional first critical buckling temperature, $\bar{T}_{cr} = T_{cr} \alpha_1 (L/h)^2$ of clamped-clamped symmetric angle-ply (15/15)_n beams, for different length to length to thickness ratios.

L/h	Number of Layers (n)				
	(15/15)	(15/15) ₂	(15/15) ₃	(15/15) ₄	(15/15) ₅
5	0.5715	0.6243	0.5980	0.6670	0.6351
10	1.3159	1.4562	1.7326	1.6967	1.7513
20	1.9436	2.1488	2.7420	2.7246	2.8394
30	2.1667	2.3482	3.0669	3.0648	3.2044
40	2.1912	2.4276	3.2007	3.2063	3.3566
50	2.2450	2.4611	3.2627	3.2732	3.5059

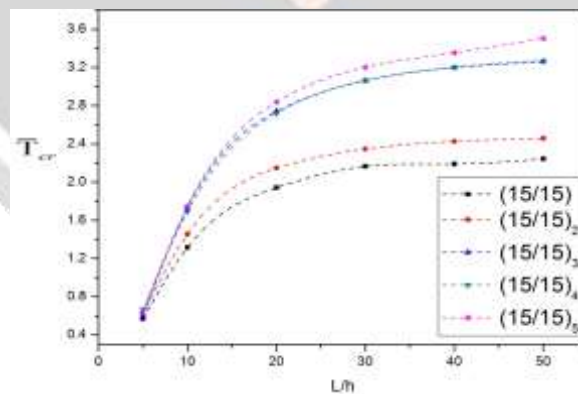


Figure 11: Effect of length to thickness ratio (L/h) on the non-dimensional first critical buckling temperature symmetric angle-ply (15/15)_n clamped-clamped beams having different number of layers.

Table 9: Non-dimensional first critical buckling temperature, $\bar{T}_{cr} = T_{cr} \alpha_1 (L/h)^2$ of clamped-clamped symmetric angle-ply (30/30)_n beams, for different length to length to thickness ratios.

L/h	Number of Layers (n)				
	(30/30)	(30/30) ₂	(30/30) ₃	(30/30) ₄	(30/30) ₅
5	1.29165	1.3044	1.378125	1.43025	1.4088
10	1.93857	2.46852	2.88789	2.92047	2.97807
20	2.15424	3.10608	3.74352	3.81936	3.90468
30	2.188944	3.26187	3.95766	4.04703	4.13937
40	2.20008	3.32832	4.044384	4.13904	4.233648

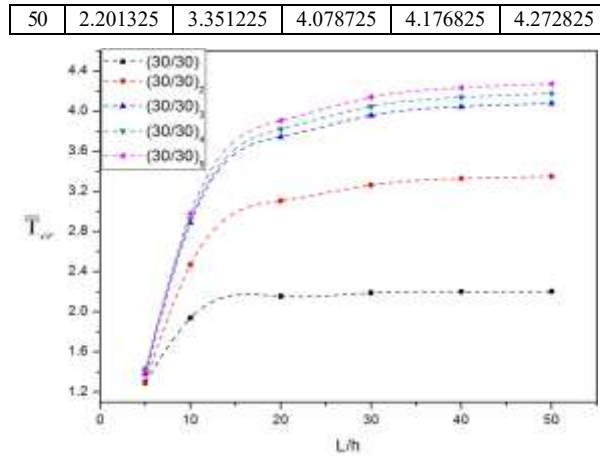


Figure 12: Effect of length to thickness ratio (L/h) on the non-dimensional first critical buckling temperature symmetric angle-ply (30/30)_n clamped-clamped beams having different number of layers.

Table 10: Non-dimensional first critical buckling temperature, $\bar{T}_{cr} = T_{cr} \alpha_1 (L/h)^2$ of clamped-clamped symmetric angle-ply (45/45)_n beams, for different length to length to thickness ratios.

L/h	Number of Layers (n)				
	(45/45) ₂	(45/45) ₃	(45/45) ₄	(45/45) ₅	(45/45) ₆
5	1.16445	1.6104	1.697775	1.716825	1.725225
10	1.50891	2.31969	2.45742	2.49597	2.50689
20	1.61676	2.59404	2.74536	2.7924	2.80296
30	1.635795	2.654208	2.80557	2.85444	2.86443
40	1.642512	2.68032	2.829312	2.878848	2.888016
50	1.644225	2.688225	2.837775	2.887725	2.89695

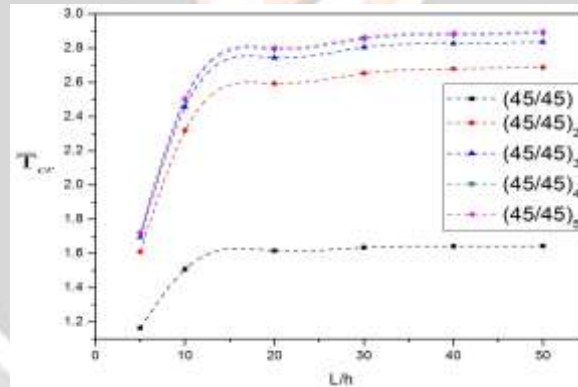


Figure 13: Effect of length to thickness ratio (L/h) on the non-dimensional first critical buckling temperature symmetric angle-ply (45/45)_n clamped-clamped beams having different number of layers.

Table 11: Non-dimensional first critical buckling temperature, $\bar{T}_{cr} = T_{cr} \alpha_1 (L/h)^2$ of clamped-clamped symmetric angle-ply (60/60)_n beams, for different length to length to thickness ratios.

L/h	Number of Layers (n)				
	(60/60) ₂	(60/60) ₃	(60/60) ₄	(60/60) ₅	(60/60) ₆
5	0.976875	1.09665	1.11675	1.121025	1.1232
10	1.21311	1.39695	1.41852	1.42509	1.42683
20	1.2894	1.49952	1.5186	1.52592	1.527
30	1.304343	1.520937	1.538757	1.546155	1.546992
40	1.309872	1.52952	1.546224	1.553664	1.554288
50	1.311975	1.532775	1.54935	1.55685	1.55745

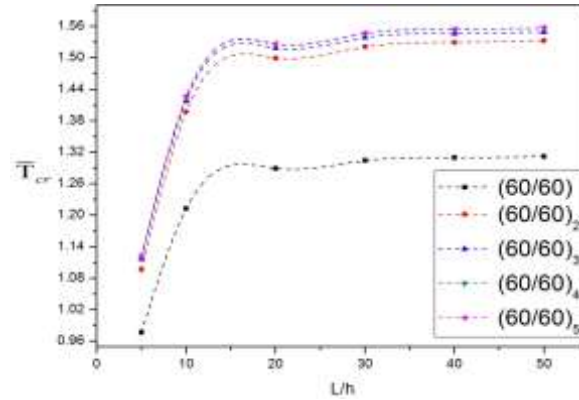


Figure 14: Effect of length to thickness ratio (L/h) on the non-dimensional first critical buckling temperature symmetric angle-ply (60/60)_n clamped-clamped beams having different number of layers.

Table 12: Non-dimensional first critical buckling temperature, $\bar{T}_{cr} = T_{cr} \alpha_1 (L/h)^2$ of clamped-clamped symmetric angle-ply (75/75)_n beams, for different length to length to thickness ratios.

L/h	Number of Layers (n)				
	(75/75) ₁	(75/75) ₂	(75/75) ₃	(75/75) ₄	(75/75) ₅
5	0.849075	0.877875	0.879975	0.880425	0.880725
10	1.0503	1.08078	1.08279	1.08378	1.0839
20	1.12104	1.147992	1.14972	1.150908	1.150944
30	1.135566	1.161783	1.163376	1.164618	1.164618
40	1.140672	1.167024	1.168512	1.16976	1.16976
50	1.1433	1.16925	1.17075	1.172025	1.17195

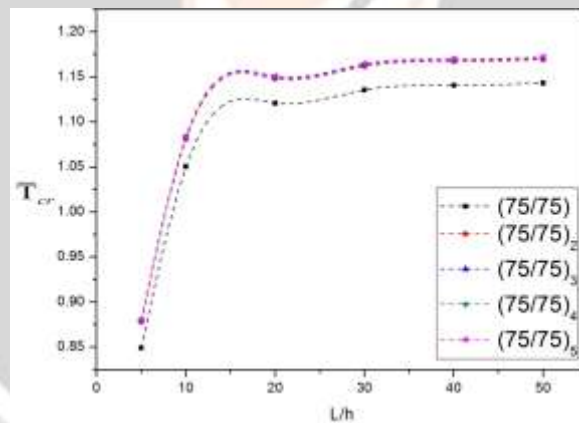


Figure 15: Effect of length to thickness ratio (L/h) on the non-dimensional first critical buckling temperature symmetric angle-ply (75/75)_n clamped-clamped beams having different number of layers.

Represents the buckling behavior of laminated composite beam as shown in figures (6-15), as the angle ply orientations of the composite beam increases the length to thickness ratios (L/h) and non-dimensional critical buckling temperatures are also increases, with increase the number of layers. The maximum number of layers is higher buckling strength as compared to minimum number of layers, by comparing symmetric and anti-symmetric angle-ply orientations of composite beams, the critical buckling temperatures are maximum angle-ply (30°) and minimum angle-ply (75°).

Table 13: Non-dimensional first critical buckling temperature, $\bar{T}_{cr} = T_{cr} \alpha_1 (L/h)^2$ of clamped-clamped anti-symmetric cross-ply (0/90)_n beams, for different modulus ratios, using (L/h=10).

E ₁ /E ₂	Number of Layers (n)				
	(0/90)	(0/90) ₂	(0/90) ₃	(0/90) ₄	(0/90) ₅
3	1.56279	1.77369	1.81218	1.81848	1.81809
10	1.12575	1.75296	1.8549	1.88967	1.9056
20	0.87555	1.51935	1.61025	1.64046	1.6542
30	0.75144	1.3173	1.38885	1.41222	1.42278
40	0.67131	1.15755	1.21833	1.23201	1.24017

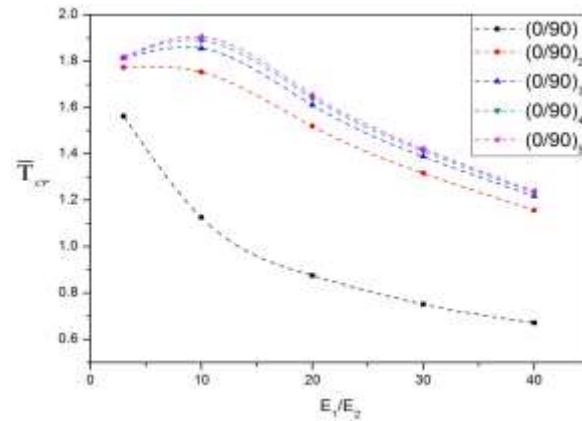


Figure 16: Effect of modulus ratio (E_1/E_2) on the non-dimensional first critical buckling temperature anti-symmetric cross-ply $(0/90)_n$ clamped-clamped beams having different number of layers.

Represents the buckling behavior of laminated composite beam as shown in figure 16, as the cross-ply orientations of the composite beam increases the modulus ratios (E_1/E_2) and non-dimensional critical buckling temperatures are decreases, with the increase number of layers, the modulus ratio is increases and buckling strength are increases. The maximum number of layers is higher buckling strength as compared to minimum number of layers.

4. CONCLUSIONS

In general the buckling load for an anti-symmetric angle-ply laminated beam is higher than anti-symmetric cross-ply laminated plate. The coupling effect decreases the magnitude of buckling load. This effect is more dominant for lesser number of layers. There is dramatic increase in buckling load with increase in laminate thickness. The buckling load decreases with an increase of aspect ratio for both cross-ply and angle-ply laminated beams. The effect of different parameters (e.g. number of layers, aspect ratio, lamination angle etc.).

5. REFERENCES

- [1] Marwah G. Kareem (Feb 2024), Thermal buckling analysis for hybrid and composite laminated plate by using new displacement function, Volume 14, Issue 1, ISSN: 2022-0597
- [2] Kapil Raj, Jyoti Vimal, Vedansh Chaturvedi (Aug 2023), Buckling Analysis of Laminated Composite Plate Using FE Method, Volume 11, Issue 8, ISSN: 2321-9653.
- [3] Fatima Zohra Kettaf, Mohamed Beguediab, Soumia Benguediab, Mahmoud M. Selim, Abdelouahed Tounsi and Muzamal Hussain (Sept 2021), Mechanical and thermal buckling analysis of laminated composite plates, Volume 40, Number 5, pages 697-708
- [4] Akbas, Seref D (Aug 2018), Thermal post-buckling analysis of a laminated composite beam, Volume 67, Issue 4, Pages.337-346, pISSN :1225-4568), eISSN :1598-6217
- [5] Houdayfa Ounis, Abdelouahab Tati and Adel Benhabane, (2014). Thermal buckling behaviour of laminated composite plates: a finite element study, *Mech. Eng.* 9(1), pp 41-49.
- [6] Rohit saha and Maiti. P. R., (2012). Buckling of simply supported FGM plates under uniaxial load, *International Journal of Civil and Structure Engineering* 2, pp 4, ISSN: 0976-4399.
- [7] M. Kamruzzaman, A.Umar, S. Q. A. Naqui and N. A. Siddique, (2006). Effect of composite type and its configuration on buckling strength of thin laminated composite plates, *Latin American Journal of Solids and Structures* 3, pp 279-299.
- [8] Erdogan Madenci and Ibrahim Guven, (2006). *The Finite Element Method and Applications in Engineering Using ANSYS*, University of Arozona, ISBN-0387282890.
- [9] A. A. Khdeir, Riyadh and Saudi Arabia, (2001). Thermal buckling of cross-ply laminated composite beams, *Acta Mechanica* 149, pp 201-213.